Scientific paper

# Ionic Liquid Supported on Magnetic Graphene Oxide as a Highly Efficient and Stable Catalyst for the Synthesis of Triazolopyrimidines

### Azar Jahanbakhshi, Mahnaz Farahi\* and Yeganeh Aghajani

Department of Chemistry, Yasouj University, Yasouj 75918-74831, Iran

\* Corresponding author: E-mail: farahimb@yu.ac.ir

Received: 05-25-2022

#### **Abstract**

A novel sulfonic acid functionalized ionic liquid was prepared by anchoring 1-(propyl-3-sulfonate) vinylimidazolium hydrogen sulfate ( $[(CH_2)_3SO_3HVIm]HSO_4$ ) on Fe<sub>3</sub>O<sub>4</sub>@GO. The prepared heterogeneous catalyst was characterized by XRD, FT-IR, EDX, SEM, VSM and TGA techniques. The results show that  $[(CH_2)_3SO_3HVIm]HSO_4$  was successfully deposited on the surface of Fe<sub>3</sub>O<sub>4</sub>@GO and the prepared ionic liquid catalyst exhibited good thermal stability. The activity of the prepared catalyst was investigated in the synthesis of triazolo[1,5-a]pyrimidine derivatives by a one-pot three-component reaction of active methylene compound (malononitrile or ethyl cyanoacetate), 3-amine-1H-1,2,4-triazole and aryl aldehydes under solvent-free conditions. This catalyst could be rapidly separated by an external magnet and recycled seven times without significant loss of catalytic activity.

Keywords: Ionic liquid; graphene oxide; triazolopyrimidines; Fe<sub>3</sub>O<sub>4</sub>

#### 1. Introduction

Ionic liquids (ILs) are increasingly recognized as environmentally friendly materials, alternative reaction media, and promising catalysts due to their unique properties such as tunable acidity, selective solubility, negligible vapor pressure, wide liquid range, and high thermal stability.<sup>1,2</sup> Ionic liquids have been developed for various specialty applications such as catalysts, fossil fuel desulfurization reagents, lubricants, and as monomers for the synthesis of ionic polymers. They are also known as "versatile chemicals" in various fields of synthetic chemistry.<sup>3,4</sup> Among them, the acidic ionic liquids functionalized with sulfonic acid groups with a hydrogen sulfate counteranion have been intensively studied as a class of dual acid functionalized ILs because both the SO<sub>3</sub>H functional groups and the hydrogen sulfate counteranion can increase their acidity. Despite the advantages of ionic liquids, their widespread use was still hindered by some disadvantages, such as intolerable viscosity, complex product isolation and catalyst recovery, high cost, and long reaction times.<sup>5,6</sup> Immobilization of ionic liquids on various solid supports is one of the most efficient ways to overcome these problems. Ionic liquids on supports have the advantage of combining the properties of an ionic liquid with the typical advantag-

es of immobilization, such as easy recycling and improved selectivity in applications with catalytic activity.<sup>7</sup> Heterogenization of ionic liquids on suitable porous supports,<sup>8–10</sup> suitable magnetic nanoparticles, 11-13 immobilized on solid supports, either by physical coating of the ionic liquids on  $Al_2O_3$ , <sup>14,15</sup>  $SiO_2$  <sup>16,17</sup> and  $TiO_2$  <sup>18,19</sup> or by covalent bonding of the ionic liquids to the support surface, would be a feasible and attractive approach to prepare an efficient solid catalyst with superior activity and stability.<sup>20</sup> While reasonable reusability was observed in most cases, the dispersion of the ionic liquid on the solid support was poor, and leaching of the ionic liquid occurred, resulting in loss of activity. 21,22 To overcome these drawbacks, graphene oxide (GO) can be used as a support material for immobilization of the ionic liquid with better dispersion, excellent activity, covalent bonding, and good reusability. In general, graphene oxide has some oxygen-containing functions (such as epoxy, carboxy and hydroxy groups). Therefore, it could be a promising candidate as an advantageous support for the immobilization of ILs. <sup>23–27</sup> ILs on graphene oxide supports have advantages due to their physicochemical properties; nevertheless, it is the tedious and time-consuming separation procedures that limit their practical applications. In this context, the development of magnetic graphene oxide as a support material has shown promise.<sup>28–31</sup>

In recent years, green chemistry has become one of the most important aspects of experimental and industrial efforts of chemists. Due to their high atomic efficiency and significant diversity, multicomponent reactions (MCRs) have occupied an essential place in the world of green chemistry. 32-34 The multicomponent reaction is a powerful synthetic strategy in modern chemistry in which three or more simple components are involved as starting reagents in a one-pot system to obtain new complex molecules with lower processing costs compared to the stepwise method, which usually produces few byproducts. Multicomponent reactions are an advantageous tool for the synthesis of critical heterocyclic compounds that have many biological activities. 35-37 The pyrimidine family is the most important nitrogen-containing heterocycle because it is found in many natural and biologically active products. It is known that the condensation of triazole and pyrimidine leads to the formation of bicyclic heterocycles known as triazolopyrimidines, which exhibit a wide range of biological properties.<sup>38-40</sup> Triazolopyrimidines can be used in a variety of synthetic pharmacophores. In addition, they are valuable building blocks for the structure of many herbicides such as penoxsulam, diclosulam, flumetsulam, azafenidin, and floransulan.41-45 Furthermore, triazolopyrimidines are synthetic analogs of purines and nucleosides. Also, [1,2,4]triazolo[1,5-a]pyrimidines, a subtype of bioisosteric purine analogs, have been reported to possess potential antitumor activities, particularly those bearing functional groups at C-5, C-6, or C-7 positions. 46,47 Several synthetic strategies have been described for the preparation of triazolopyrimidine derivatives, most of which are based on a modification of the classical Biginelli reaction. 48,49 Although some of these procedures are efficient, some of them have limiting factors, including long reaction times, side reactions, rigid workup, high-temperature conditions, and nonrecyclable reagents.

Continuing our efforts to establish an environmentally friendly method for the synthesis of reusable catalysts, <sup>50–59</sup> we report a novel magnetic graphene oxide supported by a doubly acidic ionic liquid and the catalytic activities in the synthesis of triazolo[1,5-a]pyrimidine derivatives.

## 2. Experimental

All solvents, reagents, and chemicals were purchased from Sigma-Aldrich, Merck, and Fluka chemical companies. X-ray diffraction analyzes were recorded using a Philips X Pert Pro X diffractometer operated with a Ni-filtered Cu-Ka radiation source. XRD diffraction patterns were obtained from  $2\theta = 10-80^{\circ}$ . The EDS was performed using the TESCAN-Vega model. Scanning electron micrographs were performed using a SEM: KYKY-EM3200 instrument. Thermogravimetric analysis was performed with a Perkin Elmer STA 6000 instrument in the temperature range 25–900 °C under air atmosphere. Vibration-

al sample magnetometry of magnetic materials was performed using a Kavir Magnet VSM. The IR spectrum was recorded in the range 400–4000 cm $^{-1}$  using a FT-IR JAS-CO 6300D instrument.  $^{1}$ H and  $^{13}$ C NMR spectra were recorded with a Bruker Ultrashield spectrometer (400 MHz) using DMSO- $d_6$  as solvent.

#### Preparation of [(CH<sub>2</sub>)<sub>3</sub>SO<sub>3</sub>H-VIm]HSO<sub>4</sub> (IL)

First, a mixture of 1-vinylimidazole (9.4 g) and 1,4-butanesultone (12.4 g) was stirred at room temperature for 24 hours. Then the obtained white solid was collected, washed with diethyl ether and dried at 50 °C. The prepared material was dissolved in  $\rm H_2O$  (5 ml) in a 100-ml round bottom flask, and equimolar  $\rm H_2SO_4$  was added dropwise at 0 °C. After the addition was completed, the mixture was stirred at 50 °C for 12 h, during which the ionic liquid was formed. Finally, the ionic liquid was repeatedly washed with diethyl ether and dried in vacuo at 50 °C.²

#### Synthesis of graphene oxide (GO)

Graphene oxide was synthesized using graphite powders by the modified Hummer method. In a typical synthesis procedure, graphite powder (3 g) was added to a mixture of concentrated H<sub>2</sub>SO<sub>4</sub> (12 ml), K<sub>2</sub>S<sub>2</sub>O<sub>8</sub> (2.5 g), and P<sub>2</sub>O<sub>5</sub> (2.5 g) in a beaker containing 500 ml and stirred at 80 °C for 5 hours. The mixture was then cooled to room temperature, diluted with deionized water, and stirred at room temperature for 24 hours. The mixture was then filtered, washed with deionized water and ethanol, and dried. After drying, the resulting powder was dissolved in H<sub>2</sub>SO<sub>4</sub> (120 ml) and KMnO<sub>4</sub> (15 g) in an ice bath and stirred until complete dissolution. Deionized water (250 ml) was added slowly with stirring and then heated at 35 °C for 2 hours. The reaction was then stopped by adding deionized water (250 ml) and finally hydrogen peroxide (20 ml, 30%). The resulting mixture was washed several times with aqueous HCl solution (1:10) in a centrifuge and then dried in an oven at 60 °C. Finally, the graphite oxide was sonicated in deionized water for 1 h to obtain graphene oxide nanosheets.60

#### Preparation of magnetic Fe<sub>3</sub>O<sub>4</sub> nanoparticles (MNPs)

To synthesize magnetic  $Fe_3O_4$  nanoparticles,  $Fe-Cl_3.6H_2O$  (2.7 g, 10 mmol) and  $FeCl_2.4H_2O$  (1 g, 5 mmol) were first dissolved in deionized water (45 ml) under  $N_2$  atmosphere at 80 °C for 30 min. In the next step, NaOH solution (10 ml, 25%) was slowly added dropwise until the color darkened, and then stirred for 1 h. Finally, the black product of magnetic  $Fe_3O_4$  nanoparticles was collected with an external magnet, washed with deionized water and ethanol, and dried. $^{52}$ 

#### Synthesis of Fe<sub>3</sub>O<sub>4</sub>@GO nanocomposite

The nanocomposite  $Fe_3O_4@GO$  was synthesized by the liquid self-assembly method. In a typical synthesis, GO (50 mg) was dispersed in DMF (5 ml) by ultrasonication

for two hours, and then  ${\rm Fe_3O_4}$  (40 mg) was slowly added dropwise in chloroform (10 ml). The mixture was sonicated for 4 hours at room temperature. The black colored  ${\rm Fe_3O_4@GO}$  nanocomposite was separated with an external magnet, washed with deionized water and ethanol, and finally dried.

#### Preparation of Fe<sub>3</sub>O<sub>4</sub>@GO-Pr-SH

For the functionalization of  $Fe_3O_4@GO$  nanocomposites, 3-mercaptopropyltrimethoxysilane (2 ml) was added to  $Fe_3O_4@GO$  (1 g) in dry toluene (30 ml), and the mixture was stirred under  $N_2$  atmosphere and refluxed for 24 h. The resulting product ( $Fe_3O_4@GO$ -Pr-SH) was separated by an external magnet, washed with distilled water and ethanol, and dried.

#### Synthesis Fe<sub>3</sub>O<sub>4</sub>@GO-Pr-S/IL (1)

To prepare an acidic ionic liquid on modified GO (nanocatalyst 1), a mixture of Fe $_3$ O $_4$ @GO-Pr-SH (1 g), [(CH $_2$ ) $_3$ SO $_3$ H-VIm]HSO $_4$  (5 ml), and azobisisobutyronitrile (AIBN) (5 mol%) was refluxed in toluene (100 mL) for 30 h under N $_2$  atmosphere. The catalyst was then separated with an external magnet, washed several times with diethyl ether, and then dried at 50 °C.

# General procedure for the synthesis of triazolopyrimidines 5

To a mixture of aldehyde (1 mmol), ethyl cyanoacetate or malononitrile (1 mmol), and 3-amine-1H-1,2,4-triazole (1 mmol) was added catalyst 1 (0.004 g) under solvent-free conditions at 80 °C. The reaction progress was monitored by TLC (n-hexane/EtOAc). After completion of the process, EtOAc (10 ml) was added and the Fe<sub>3</sub>O<sub>4</sub>@ GO-Pr-S/IL-nanocatalyst was separated using an external magnet. Further purification of the product was performed by recrystallization from EtOH.

#### General procedure for the recovery of nanocatalyst 1

Recovery of Fe $_3$ O $_4$ @GO-Pr-S/IL was carried out in the synthesis of pyrimidine derivatives. The mixture of benzaldehyde (1 mmol), ethyl cyanoacetate or malononitrile (1 mmol) and 3-amine-1H-1,2,4-triazole (1 mmol) was stirred in the presence of catalyst 1 (0.004 g) under optimum conditions. After completion of the reaction, hot EtOAc (10 ml) was added and the nanocatalyst was separated from the reaction mixture using an external magnet. Then, the recovered catalyst was washed several times with EtOAc (10 ml) and deionized water (10 ml) and dried. Finally, the recovered catalyst was reused seven times consecutively under the same conditions.

#### Selected spectral data

Ethyl 5-amino-7-phenyl-1,7-dihydro-[1,2,4]triazolo [1,5-*a*]pyrimidine-6-carboxylate (**5a**). FT-IR (KBr, cm<sup>-1</sup>) v 3396, 3375, 3326, 2746, 1687, 1565, 1490, 1110; <sup>1</sup>H NMR (400 MHz, DMSO- $d_6$ )  $\delta$  9.25 (s, 1H), 8.08 (d, 1H, J = 8 Hz),

7.66 (s, 2H), 5.37 (s, 1H), 3.93 (q, 2H, J = 8 Hz), 0.84 (t, 3H, J = 8 Hz), 7.57–7.64 (m, 5H) ppm.

Ethyl 5-amino-7-(4-chlorophenyl)-4,7-dihydro-[1,2,4]triazolo[1,5-a]pyrimidine-6-carboxylate (**5b**). FT-IR (KBr, cm<sup>-1</sup>) v 3412, 3253, 3115, 2872, 1692, 1532, 1485, 1203;  $^{1}$ H NMR (400 MHz, DMSO- $d_6$ )  $\delta$  9.25 (s, 1H), 8.08 (d, 1H, J = 8 Hz), 7.65 (s, 2H), 5.41 (s, 1H), 4.38 (q, 2H, J = 7 Hz), 0.92 (t, 3H, J = 7 Hz), 7.45–7.58 (m, 5H);  $^{13}$ C NMR (100 MHz, DMSO- $d_6$ )  $\delta$  163.83, 160.63, 154.82, 134.82, 130.96, 129.87, 129.04, 110.16, 61.09, 57.01, 14.02.

Ethyl 5-amino-7-(4-bromophenyl)-4,7-dihydro-[1,2,4]triazolo[1,5-a]pyrimidine-6-carboxylate (**5c**). FT-IR (KBr, cm<sup>-1</sup>) v 3427, 3389, 3098, 2923, 1677, 1587, 1488, 1178;  $^{1}$ H NMR (400 MHz, DMSO- $d_6$ ) δ 9.16 (s, 1H), 7.08 (d, 1H, J= 3.6 Hz), 8.39 (s, 2H), 5.21 (s, 1H), 3.98 (q, 2H, J=6.4 Hz), 1.33 (t, 3H, J= 6.6 Hz), 7.41–7.43 (m, 5H);  $^{13}$ C NMR (100 MHz, DMSO- $d_6$ ): δ = 169.6, 156, 146, 141.99, 132.5, 129, 126.8, 62.1, 40.6, 27.5.

Ethyl 5-amino-7-(4-nitrophenyl)-4,7-dihydro-[1,2,4]triazolo[1,5-a]pyrimidine-6-carboxylate (5**d**). FT-IR (KBr, cm<sup>-1</sup>) ν 3480, 3430, 3198, 2917, 1680, 1604, 1504, 1054; <sup>1</sup>H NMR (400 MHz, DMSO- $d_6$ ) δ 13.99 (s, 1H), 8.10 (d, 1H, J = 8 Hz), 7.83–7.91 (m, 4 H), 5.99 (s, 1H), 4.43 (q, 2H, J = 7.2 Hz), 1.03 (t, 1H, J = 3.2 Hz); <sup>13</sup>C NMR (100 MHz, DMSO- $d_6$ ) δ 163.62, 154.95, 149.60, 144.21, 134.01, 131.06, 130.42, 124.86, 124.46, 114.11, 63.57, 59.84, 14.00.

Ethyl 5-amino-7-(3-nitrophenyl)-1,7-dihydro-[1,2,4]triazolo[1,5-a]pyrimidine-6-carboxylate (**5e**). FT-IR (KBr, cm<sup>-1</sup>) ν 3444, 3328, 3097, 2888, 1697, 1623, 1531, 1272; <sup>1</sup>H NMR (400 MHz, DMSO- $d_6$ ) δ 6.41 (s, 1H), 8.09 (d, 1H, J = 8 Hz), 7.80–7.83 (m, 5H), 5.69 (s, 1H), 4.03 (q, 2H, J = 8 Hz), 0.92 (t, 3H, J = 8 Hz); <sup>13</sup>C NMR (100 MHz, DMSO- $d_6$ ) δ 163.63, 154.55, 150.36, 147.93, 134.84, 131.17, 130.83, 125.30, 123.78, 123.13, 113.63, 63.19, 59.06, 13.86.

Ethyl 5-amino-7-(2,4dichlorophenyl)-1,7-dihydro-[1,2,4]triazolo[1,5-a]pyrimidine-6-carboxylate (**5f**). FT-IR (KBr, cm<sup>-1</sup>) v 3489, 3421, 3085, 2878, 1699, 1586, 1474, 1106; <sup>1</sup>H NMR (400 MHz, DMSO- $d_6$ ) δ 11.67 (s, 1H), 8.11 (d, 1H, J = 8 Hz), 7.87 (s, 2H), 4.16 (s, 1H), 2.48 (q, 2H, J = 8 Hz), 1.25 (t, 3H, J = 7 Hz), 7.26–7.77 (m, 5H); <sup>13</sup>C NMR (100 MHz, DMSO- $d_6$ ) δ 160.6, 153.6, 137.6, 130.2, 120.8, 127, 67.1, 40.4, 21.6.

Ethyl 5-amino-7-(4-methylphenyl)-7,8-dihydro-[1, 2,4]-triazolo[4,3-a]pyrimidine-6-carbonitrile (**5g**). FT-IR (KBr, cm<sup>-1</sup>) v 3347, 3262, 3185, 3118, 2921, 2192, 1660, 1633, 1531, 1482, 1363, 1286, 1214, 1157;  $^1$ H NMR (400 MHz, DMSO- $d_6$ )  $\delta$  2.28 (s, 3H), 5.29 (d, 1H, J = 2.4 Hz), 7.18 (s, 4H), 7.21 (s, 2H), 7.71 (s, 1H), 8.75 (d, 1H, J = 1.6 Hz);  $^{13}$ C NMR (100 MHz, DMSO- $d_6$ )  $\delta$  20.64, 53.70, 56.06, 119.06, 126.00, 129.18, 137.26, 140.24, 146.93, 151.83, 153.92.

Ethyl 5-amino-7-(4-isopropylphenyl)-7,8-dihydro-[1,2,4]-triazolo[4,3-a]pyrimidine-6-carbonitrile (**5h**). FT-IR (KBr, cm $^{-1}$ ) v 3378, 3295, 3181, 3118, 2964, 2186, 1656, 1627, 1523, 1479, 1367, 1284, 1211, 1151;  $^{1}$ H NMR (400 MHz, DMSO- $d_6$ )  $\delta$  1.23 (d, 6H, J = 6.8 Hz), 2.92 (s, 1H),

5.33 (d, 1H, J = 2Hz), 7.24 (s, 4H), 7.31 (s, 2H), 7.76 (s, 1H), 8.80 (d, 1H, J = 1.6 Hz); <sup>13</sup>C NMR (100 MHz, DM-SO- $d_6$ )  $\delta$  23.81, 33.11, 53.68, 55.97, 119.11, 125.99, 126.59, 140.71, 146.95, 148.21, 151.83, 153.91.

#### 3. Results and Discussion

The procedure for preparing the nanocatalyst  $Fe_3O_4@GO-Pr-S/IL$  (1) is shown in Scheme 1. Bronsted's acidic ionic liquid  $[(CH_2)_3SO_3HVIm]HSO_4$  synthesized by the reaction of 1-vinylimidazole with 1,4-butanesultone followed by treatment with sulfuric acid. Subsequently, a  $Fe_3O_4@GO$ -nanocomposite was prepared and functionalized with 3-mercaptopropyltrimethoxysilane (MPTMS) via covalent bonds to prepare  $Fe_3O_4@GO-Pr-SH$ . Finally,  $Fe_3O_4@GO-Pr-S/IL$  nanocatalyst 1 was obtained by the reaction of  $[(CH_2)_3SO_3HVIm]HSO_4$  and  $Fe_3O_4@GO-Pr-SH$  in the presence of azobisisobutyronitrile (AIBN) in toluene under  $N_2$  atmosphere. After successful synthesis of  $Fe_3O_4@GO-Pr-S/IL$ , the structure of this new nanocatalyst was characterized by XRD, EDS, FT-IR, VSM, SEM and TGA techniques.

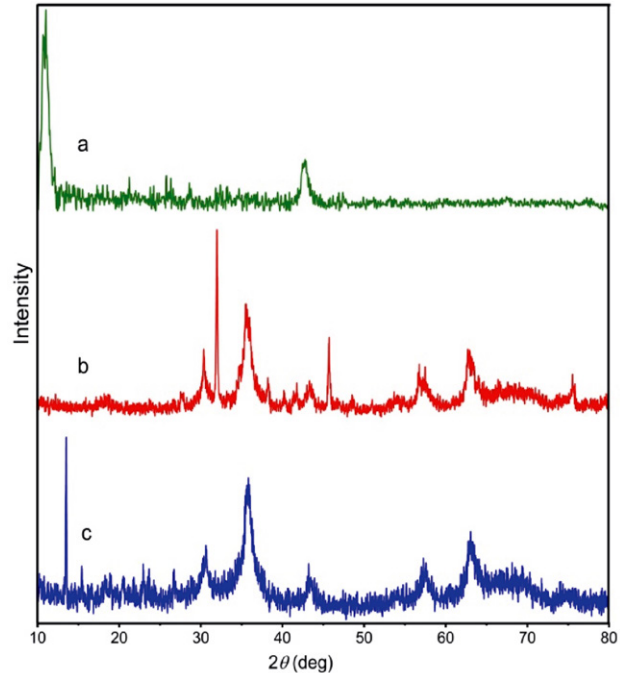


**Figure 1.** XRD patterns of a) GO, b) Fe<sub>3</sub>O<sub>4</sub>, and c) Fe<sub>3</sub>O<sub>4</sub>@GO-Pr-S/

**Scheme 1.** Preparation of Fe<sub>3</sub>O<sub>4</sub>@GO-Pr-S/IL (1).

Figure 1 shows the X-ray diffraction spectroscopy patterns of GO,  $Fe_3O_4$ , and  $Fe_3O_4$ @GO-Pr-S/IL. The peaks at  $2\theta = 10.5^\circ$  and  $43.5^\circ$  could correspond to the (01) and (101) layers of GO, respectively.  $^{62,63}$  In Figure 1b, the peaks at  $30.26^\circ$ ,  $35.7^\circ$ ,  $43.5^\circ$ ,  $53.59^\circ$ ,  $57.5^\circ$ , and  $63.26^\circ$  relate to (220), (311), (400), (422), (511), and (440) free  $Fe_3O_4$ , respectively, which agrees well with the pattern of  $Fe_3O_4$ .  $^{64,65}$  After grafting various functional groups onto GO (Figure 1c), the 001 diffraction peak of GO completely disappeared, indicating complete exfoliation of GO and preventing the aggregation of GO after partial reduction. Moreover, the  $Fe_3O_4$ @GO-Pr-S/IL nanocatalyst shows characteristic peaks at  $2\theta$ , which are consistent with the bare peaks of  $Fe_3O_4$ .

Elemental analysis of  $Fe_3O_4@GO$ -Pr-S/IL was performed by EDX analysis (Figure 2). The EDX spectrum proves the presence of the common elements C, O, Fe, N, Si and S in the catalyst structure as shown.

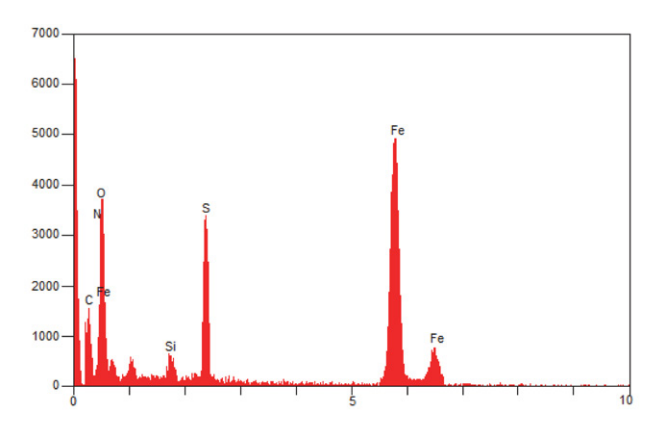
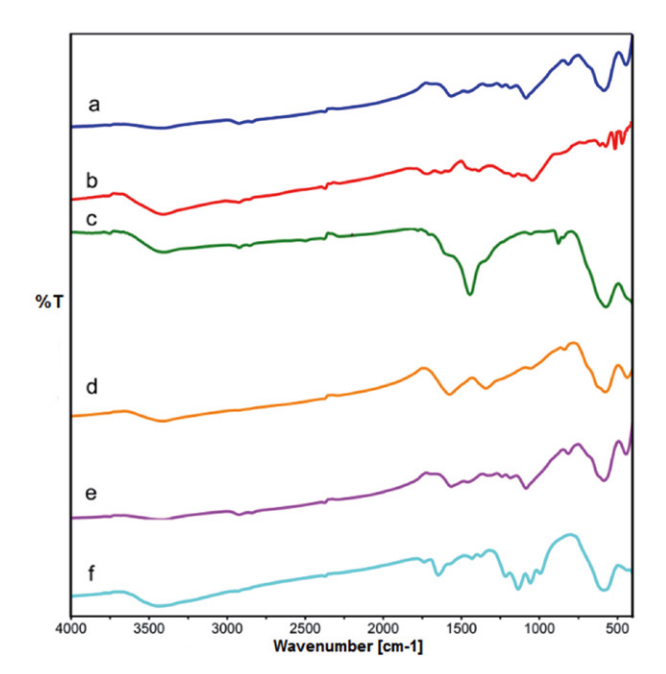


Fig. 2. EDS diagram of Fe<sub>3</sub>O<sub>4</sub>@GO-Pr-S/IL.

In Figure 3a, three absorption peaks at about 645, 1050, and 1135 cm<sup>-1</sup> are associated with the vibrations of the S-O, SO<sub>2</sub>, and C-S bands, respectively. In addition, the characteristic peaks of the imidazolium ring at 1563 cm<sup>-1</sup> were observed (Figure 3a).<sup>66-68</sup> The FT-IR spectra of GO are shown in Figure 3b. The peak at 1227 cm<sup>-1</sup> is assigned to the stretching vibration of C-O of the epoxide group, and the peak of C=O of the carboxyl and carbonyl groups is at 1724 cm<sup>-1</sup> (Figure 3b).<sup>69,70</sup> The strong peak in all spectra at 3400 cm<sup>-1</sup> corresponds to the OH group (Figure 3b-f). In Fe<sub>3</sub>O<sub>4</sub>@GO-Pr-S/IL this peak (OH group) is much more pronounced than in Fe<sub>3</sub>O<sub>4</sub>@ GO-Pr-SH due to the sulfonic acid groups. Moreover, the typical peak at 580 cm<sup>-1</sup> in all spectra (Figure 3c-f) can be attributed to Fe-O stretching.<sup>71</sup> In addition, symmetric and asymmetric vibrations of the Si-O bond occur at about 973 and 1140 cm<sup>-1</sup>, confirming the presence of MPTMS (Figure 3d).<sup>72</sup> The presence of all these peaks indicates the successful association of the Bronsted ionic acid liquid with the Fe<sub>3</sub>O<sub>4</sub>@GO-Pr-SH via a radical reaction.



**Figure 3.** FT-IR spectra of a) IL, b) GO, c)  $Fe_3O_4$ , d)  $Fe_3O_4$ @GO, e)  $Fe_3O_4$ @GO-Pr-SH, and f)  $Fe_3O_4$ @GO-Pr-S/IL.

The magnetic property of  $Fe_3O_4$  and  $Fe_3O_4@GO-Pr-S/IL$  nanocatalysts was determined by VSM at room temperature (Figure 4). The curves in Figure 4 show that the saturation magnetization values of  $Fe_3O_4@GO-Pr-S/IL$  (20.55 emu/g) are lower than those of pure  $Fe_3O_4$  nanoparticles (53.03 emu/g). The decrease in saturation magnetization of  $Fe_3O_4@GO-Pr-S/IL$  nanocatalyst might be related to the functionalized GO and the presence of an acid group on the surface of the ionic liquid associated with the support.

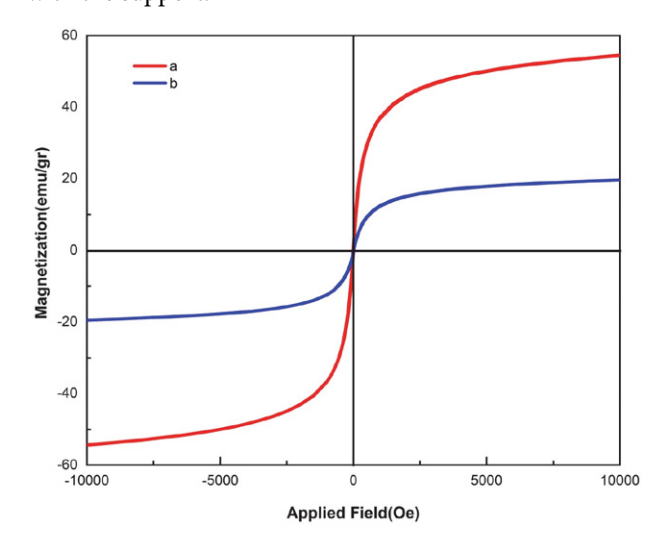


Figure 4. VSM analysis of a) Fe<sub>3</sub>O<sub>4</sub> and b) Fe<sub>3</sub>O<sub>4</sub>@GO-Pr-S/IL.

The morphology and size of the nanocatalysts GO and Fe $_3$ O $_4$ @GO-Pr-S/IL were studied using SEM (Figure 5). GO has a 2D structure with a wrinkled edge and a large

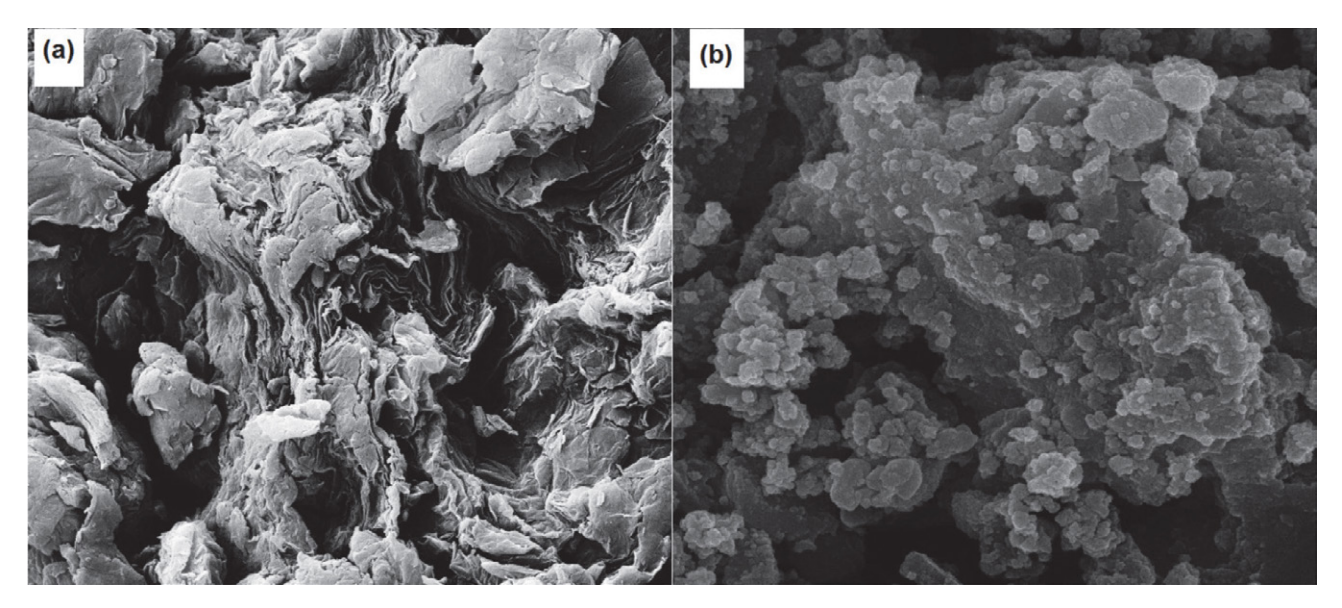


Figure 5. SEM images of a) GO and b) Fe<sub>3</sub>O<sub>4</sub>@GO-Pr-S/IL.

thickness (Figure 5a). However, after immobilization of the ionic liquid, the surface of GO is smooth (Figure 5b). According to this picture, the average particle size is 77–90 nm, and the surface of the nanocatalyst is almost uniform.

The thermal stability of the Fe $_3$ O $_4$ @GO-Pr-S/IL nanocatalyst was also investigated by thermogravimetric analysis (TGA) (Figure 6). The TGA curve of nanocatalyst 1 shows three stages of weight loss between 25 and 900 °C. In this curve, the first weight loss below 220 °C (18%) is due to desorption of chemisorbed and physically adsorbed solvents, organic solvents, and hydroxyl groups. The second weight loss occurs at about 220–550 °C (8%) and is due to decomposition of oxygenated groups into GO, organic groups, acid groups, and amine groups. The final weight losses occur at 550–900 °C (10%). They may be due to the removal of these immobilized organic species on the surface of GO nanosheets and confirm the thermal stability of the prepared nanocatalyst.

In the next step,  $Fe_3O_4@GO-Pr-S/IL$  was used as an effective nanocatalyst for the synthesis of triazolo[1,5-a] pyrimidine derivatives 5 (Scheme 2).

**Scheme 2.** Synthesis of triazolo[1,5-a] pyrimidine derivatives **5** in the presence of nanocatalyst **1**.

Table 1 shows the effects of catalyst amount, temperature and different solvents on the reaction between benzaldehyde (1 mmol), ethyl cyanoacetate (1 mmol) and 3-amine-1*H*-1,2,4-triazole (1 mmol) as an example reac-

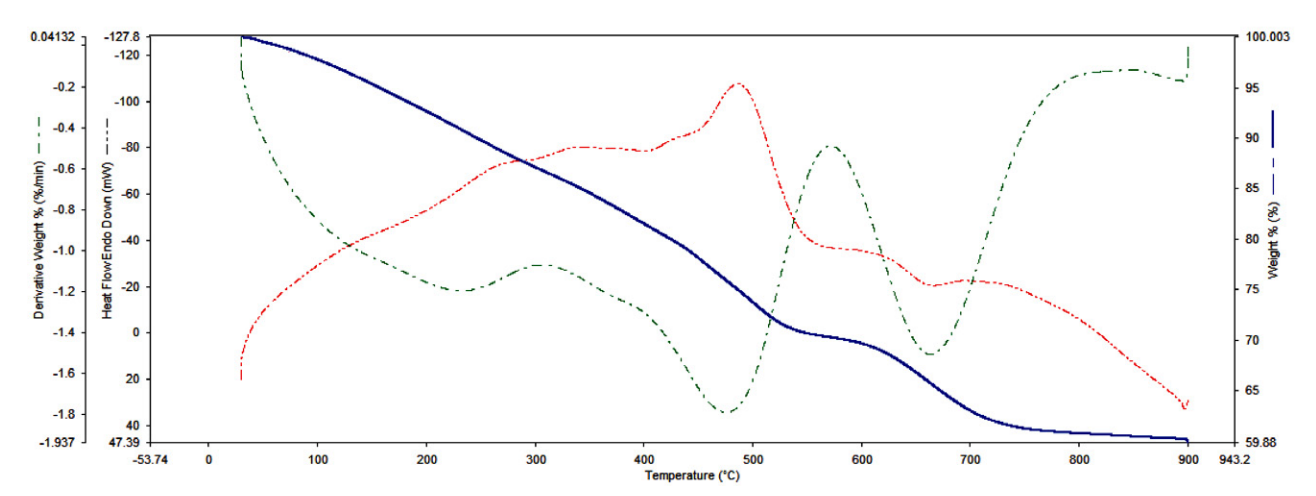


**Figure 6.** TGA curve of the Fe<sub>3</sub>O<sub>4</sub>@GO-Pr-S/IL nanocatalyst.

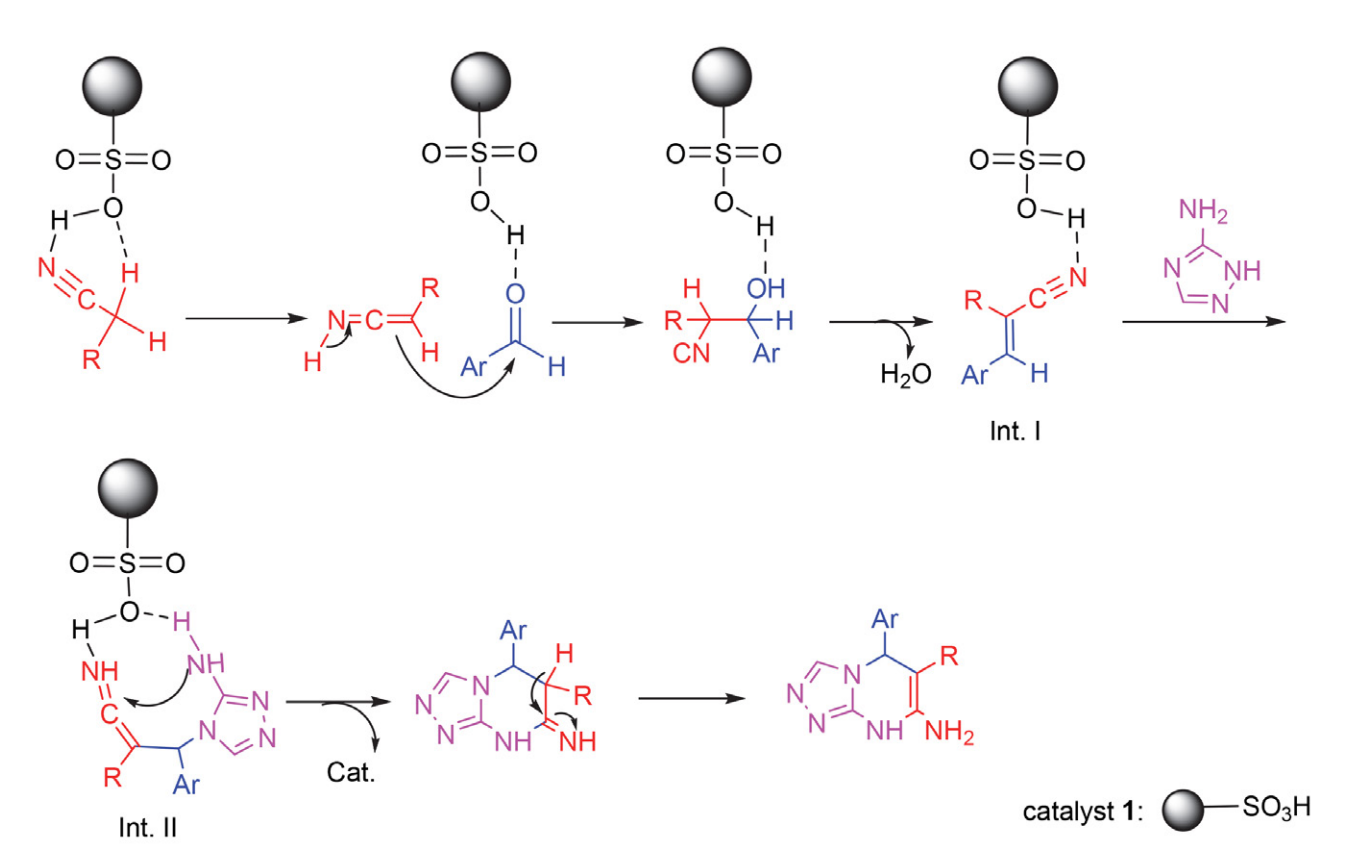
Table 1. The effect of catalyst loading, solvent and temperature in the synthesis of 5a.<sup>a</sup>

| Entry | Catalyst 1 (g | g) Solvent                         | Temp. (°C) | Yield <sup>b</sup> (%) |
|-------|---------------|------------------------------------|------------|------------------------|
| 1     | 0.002         | _                                  | 25         | 62                     |
| 2     | 0.002         | _                                  | 60         | 70                     |
| 3     | 0.002         | -                                  | 80         | 80                     |
| 4     | 0.001         | -                                  | 80         | 65                     |
| 5     | 0.004         | -                                  | 80         | 95                     |
| 6     | 0.006         | -                                  | 80         | 90                     |
| 7     | 0.008         | _                                  | 80         | 90                     |
| 8     | 0.004         | EtOH                               | 80         | 80                     |
| 9     | 0.004         | CH <sub>3</sub> CN                 | 80         | 82                     |
| 10    | 0.004         | Toluene                            | 80         | 70                     |
| 11    | 0.004         | $H_2O$                             | 80         | 65                     |
| 12    | 0.004         | H <sub>2</sub> O/EtOH (1:1         | ) reflux   | 75                     |
| 13    | 0.004         | GO                                 | 80         | 37                     |
| 14    | 0.004         | $Fe_3O_4$                          | 80         | 45                     |
| 15    | 0.004         | Fe <sub>3</sub> O <sub>4</sub> @GO | 80         | 57                     |
| 16    | -             | _                                  | 80         | trace                  |

 $<sup>^{\</sup>rm a}$  Reaction conditions: benzaldehyde (1 mmol), ethyl cyanoacetate (1 mmol), 3-amine-1*H*-1,2,4-triazole (1 mmol), time: 20 min.  $^{\rm b}$  Isolated yields.

tion. The model reaction was carried out at different temperatures, and the best yield was obtained at 80 °C. We optimized the amount of catalyst; the maximum yield of the product was obtained with 0.004 g of catalyst under solvent-free conditions. The yield of the product was highest when the reaction proceeded under solvent-free conditions, and when EtOH, MeCN, toluene, H2O, and H2O/ EtOH (1:1) were used as solvents, the yield of the product decreased. When GO, Fe3O4 and Fe3O4@GO were used as catalysts under solvent-free conditions at 80 °C, the product yield was much lower. The reaction did not proceed without catalyst (Table 1, entry 16), indicating that the catalyst was necessary to promote the reaction. After optimizing the reaction conditions, the efficiency of the Fe<sub>3</sub>O<sub>4</sub>@GO-Pr-S/IL nanocatalyst was further tested in the synthesis of triazolo[1,5-a]pyrimidines using a series of aromatic aldehydes and malononitrile. The results are shown in Table 2, and it was found that almost all substrates gave excellent yields of the desired products in a short reaction time.

A permissible mechanism for the three-component synthesis of triazolo[1,5-*a*]pyrimidines 5 based on previous reports is shown in Scheme 3.<sup>73,74</sup> First, the aldehyde and active methylene compounds (cyanoacetate or malononitrile) are activated with the acidic surface of the catalyst, and a Knoevenagel condensation to intermediate I occurs. Subsequently, intermediate I reacts with 3-amine-1*H*-1,2,4-triazole to give the intermediate II (via Michael addition). Finally, the desired product was synthesized after intramolecular cyclization and tautomerization.



Scheme 3. Proposed mechanism for the synthesis of 5 in the presence of Fe<sub>3</sub>O<sub>4</sub>@GO-Pr-S/IL as catalyst.

 $\textbf{Table 2.} \ \ \textbf{Synthesis of triazolo} \ [1,5-a] \textbf{pyrimidines in the presence of Fe} \\ \textbf{3O}_4 @ \textbf{GO-Pr-S/IL nanocatalyst.} \\ \textbf{a} \\ \textbf{b} \\ \textbf{a} \\ \textbf{b} \\ \textbf{c} \\ \textbf{a} \\ \textbf{c} \\ \textbf{d} \\ \textbf{d$ 

| ,   |  | J 4-   | ,  |
|---|--|--|--|
| Aldehyde  | Product 5  | Yield (%) <sup>b</sup>   | Mp (°C)  |
| C <sub>6</sub> H <sub>4</sub> CHO                     | N CO <sub>2</sub> Et   | 95   | 189–191°   |
| 4-Cl C <sub>6</sub> H <sub>4</sub> CHO                | CI<br>CO <sub>2</sub> Et<br>N NH <sub>2</sub>  | 97   | 190–191 <sup>70</sup>  |
| 4-Br C <sub>6</sub> H <sub>4</sub> CHO                | Br<br>CO <sub>2</sub> Et<br>NH <sub>2</sub>  | 93   | 184-184 <sup>70</sup>  |
| 4-NO <sub>2</sub> C <sub>6</sub> H <sub>4</sub> CHO   | NO <sub>2</sub> CO <sub>2</sub> Et   | 95   | 194–196 <sup>70</sup>  |
| 3-NO <sub>2</sub> C <sub>6</sub> H <sub>4</sub> CHO   | NO <sub>2</sub> CO <sub>2</sub> Et   | 90   | 190–192°   |
| 2,4-Cl <sub>2</sub> C <sub>6</sub> H <sub>3</sub> CHO | CO <sub>2</sub> Et   | 88   | 243-245 <sup>c</sup>   |
| 4-CH <sub>3</sub> C <sub>6</sub> H <sub>4</sub> CHO   | CH <sub>3</sub>  | 85   | 243-245 <sup>71</sup>  |
| 4- <i>i</i> -Pr C <sub>6</sub> H <sub>4</sub> CHO     | CN NH <sub>2</sub>   | 84   | 218-220 <sup>c</sup>   |
| 4-NO <sub>2</sub> C <sub>6</sub> H <sub>4</sub> CHO   | NO <sub>2</sub> CN  NH  NH <sub>2</sub>  | 90   | 245-247 <sup>71</sup>  |
| 2-Cl C <sub>6</sub> H <sub>4</sub> CHO                | CI<br>CN<br>NH12   | 92   | 263-266 <sup>71</sup>  |
| 4-Br C <sub>6</sub> H <sub>4</sub> CHO                | Br<br>CN<br>NNNH2  | 89   | 264–266 <sup>71</sup>  |
| 4-Cl C <sub>6</sub> H <sub>4</sub> CHO                | CI CN NH2  | 93   | 257-258 <sup>71</sup>  |
|   | 4-Cl C <sub>6</sub> H <sub>4</sub> CHO  4-Br C <sub>6</sub> H <sub>4</sub> CHO  4-NO <sub>2</sub> C <sub>6</sub> H <sub>4</sub> CHO  3-NO <sub>2</sub> C <sub>6</sub> H <sub>4</sub> CHO  2,4-Cl <sub>2</sub> C <sub>6</sub> H <sub>3</sub> CHO  4-CH <sub>3</sub> C <sub>6</sub> H <sub>4</sub> CHO  4-i-Pr C <sub>6</sub> H <sub>4</sub> CHO  2-Cl C <sub>6</sub> H <sub>4</sub> CHO  4-Br C <sub>6</sub> H <sub>4</sub> CHO | $C_6H_4CHO$ $N_1 = 0.0, ER = $ | C <sub>6</sub> H <sub>4</sub> CHO  4-Cl C <sub>6</sub> H <sub>4</sub> CHO  4-Br C <sub>0</sub> H <sub>4</sub> CHO  4-Br C <sub>0</sub> H <sub>4</sub> CHO  3-NO <sub>2</sub> C <sub>6</sub> H <sub>4</sub> CHO  2,4-Cl <sub>2</sub> C <sub>6</sub> H <sub>3</sub> CHO  4-CH <sub>3</sub> C <sub>6</sub> H <sub>4</sub> CHO  4-Pr C <sub>6</sub> H <sub>4</sub> CHO  4-Roy C <sub>6</sub> H <sub>4</sub> CHO  5-Roy C <sub>6</sub> H <sub>4</sub> CHO  5-Roy C <sub>6</sub> H <sub>4</sub> CHO  5-Roy C <sub>6</sub> H <sub>4</sub> CHO  6-Roy C <sub>6</sub> H <sub>4</sub> CHO  6-Roy C <sub>6</sub> H <sub>4</sub> CHO  6-Roy C <sub>6</sub> H <sub>4</sub> CHO  7-Roy C <sub>6</sub> H <sub>4</sub> CHO  89 |

 $<sup>^</sup>a$  Reaction conditions: aryl aldehyde (1 mmol), ethyl cyanoacetate or malononitrile (1 mmol), 3-amine-1*H*-1,2,4-triazole (1 mmol), catalyst **1** (0.004 g), solvent-free, 80 °C.  $^b$  Isolated yields.  $^c$  New compound.

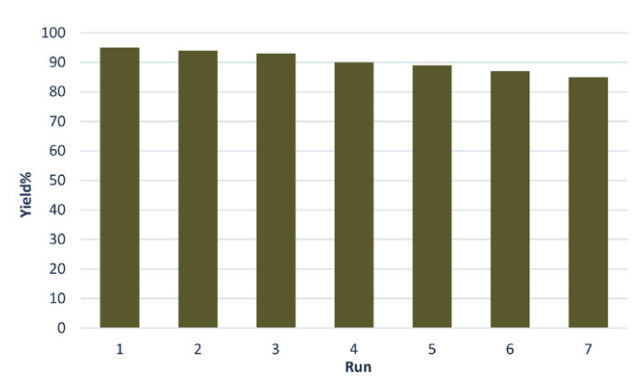


Figure 7. Reusability of the heterogeneous nanocatalyst 1 for the synthesis of 5a.

A hot filtration test was also performed to study the leaching of the catalyst during the reaction. After about 50% of the process was complete, boiling EtOAc (5 ml) was added and the catalyst was separated with a magnet. The solvent was then removed and the reaction continued under optimized conditions. Nevertheless, no remarkable increase in product conversion was observed during the course of the reaction, indicating that the catalyst func-

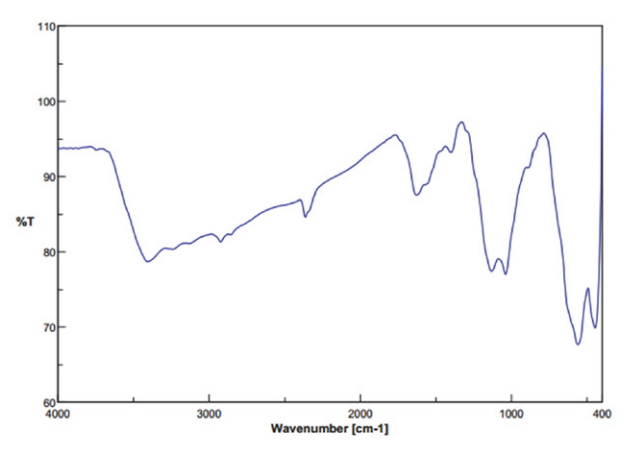


Figure 8. FT-IR spectrum of recycled Fe<sub>3</sub>O<sub>4</sub>@GO-Pr-S/IL.

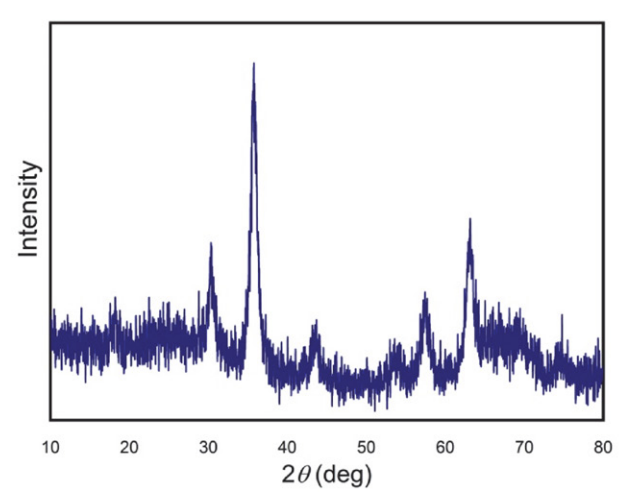


Figure 9. The XRD pattern of recycled nanocatalyst 1.

tioned as a heterogeneous method and the ionic liquid fraction was kept intact and efficient on the solid support. Moreover, the reusability of Fe<sub>3</sub>O<sub>4</sub>@GO-Pr-S/IL in the model reaction of benzaldehyde, ethyl cyanoacetate and 3-amine-1*H*-1,2,4-triazole was investigated under optimum conditions. After completion of the reaction, boiling EtOAc was added and the catalyst was separated by an external magnet, washed, and reused in subsequent runs. As shown in Figure 7, the synthesized catalyst can be recovered and reused in at least 7 runs without significant decrease in its efficiency.

In Figure 8, the FT-IR spectrum of the nanocatalyst after seven reaction cycles can be seen. This spectrum also confirms the stability of the structure of the recycled nanocatalyst. The XRD pattern also indicates the structural stability of the catalyst after being reused (Figure 9). The position and relative intensities of all peaks confirm this well.

#### 4. Conclusions

In this work, Fe<sub>3</sub>O<sub>4</sub>@GO-Pr-S/IL was prepared as a new nanocatalyst and used for the synthesis of triazolo[1,5-a]pyrimidine derivatives under green conditions, and the products were obtained in high yield. This magnetic nanocatalyst was characterized by various techniques such as XRD, FT-IR, EDX, SEM, VSM and TGA. Fe<sub>3</sub>O<sub>4</sub>@GO-Pr-S/IL was used as an efficient catalyst with good durability, high selectivity and stability, mild reaction conditions and short reaction times. The heterogeneous Fe<sub>3</sub>O<sub>4</sub>@GO-Pr-S/IL catalyst was also successfully recovered seven times, maintaining its activity.

#### 5. References

- M. Tajbakhsh, H. Alinezhad, M. Norouzi, S. Baghery, M. Akbari, *J. Mol. Liq.* 2013, 177, 44–48.
   DOI:10.1016/j.molliq.2012.09.017
- J. Miao, H. Wan, G. Guan, Catal. Commun. 2011, 12, 353–356. DOI:10.1016/j.catcom.2010.10.014
- P. Elavarasan, S. Rengadurai, S. Upadhyayula, Adv. Chem. Eng. 2020, 4, 100045–100053. DOI:10.1016/j.ceja.2020.100045
- J. Miao, H. Wan, Y. Shao, G. Guan, B. Xu, J. Mol. Catal. A Chem. 2011, 348, 77–82. DOI:10.1016/j.molcata.2011.08.005
- A. R. Hajipour, F. Rafiee, Org. Prep. Proced. Int. 2010, 42, 285–362. DOI:10.1080/00304948.2010.490177
- A. S. Amarasekara, O. S. Owereh, *Catal. Commun.* 2010, 11, 1072–1075. DOI:10.1016/j.catcom.2010.05.012
- Z. M. Li, Y. Zhou, D. J. Tao, W. Huang, X. S. Chen, Z. Yang, RSC Adv. 2014, 4, 12160–12167. DOI:10.1039/C4RA00092G
- L. T. Oliveira, R. V. Goncalves, D. V. Goncalves, D. C. S. de Azevedo, S. M. Pereira de Lucena, *J. Chem. Eng. Data* 2019, 64, 2221–2228. DOI:10.1021/acs.jced.8b01177
- 9. Q. Sun, B. Aguila, J. Perman, L. D. Earl, C. W. Abney, Y.

- Cheng, H. Wei, N. Nguyen, L. Wojtas, S. Ma, *J. Am. Chem. Soc.* **2017**, *139*, 2786–2793. **DOI**:10.1021/jacs.6b12885
- Q. Wang, S. Zhang, Y. Yu, B. Dai, Catal. Commun. 2020, 147, 106122–106142. DOI:10.1016/j.catcom.2020.106122
- M. A. Zolfigol, R. Ayazi-Nasrabadi, S. Baghery, V. Khakyzadeh, S. Azizian, *J. Mol. Catal. A: Chem.* 2016, 418, 54–67.
   DOI:10.1016/j.molcata.2016.03.027
- M. Sheykhan, L. Ma'mani, A. Ebrahimi, A. Heydari, *J. Mol. Catal. A: Chem.* 2011, 335, 253–261.
   DOI:10.1016/j.molcata.2010.12.004
- Q. Zhang, H. Su, J. Luo, Y. Wei, Green Chem. 2012, 14, 201– 208. DOI:10.1039/C1GC16031A
- 14. R. Li, Y. Jiang, J. Zhao, D. Ramella, Y. Peng, Y. Luan, *RSC. Adv.* **2017**, *7*, 34591–34597. **DOI**:10.1039/C7RA06201J
- M. Khoshnevis, A. Davoodnia, A. Zare-Bidaki, N. Tavakoli-Hoseini, Synth. React. Inorg. Met. 2013, 43, 1154–1161. DOI:10.1080/15533174.2012.756897
- M. L. Testa, V. La Parola, A. M. Venezia, *Catal. Today* 2010, 158, 109–113. DOI:10.1016/j.cattod.2010.05.027
- 17. K. Niknam, A. Deris, F. Naeimi, F. Majleci, *Tetrahedron Lett.* **2011**, *52*, 4642–4645. **DOI**:10.1016/j.tetlet.2011.06.105
- 18. S. V. Atghia, S. Sarvi-Beigbaghlou., *J. Appl. Organomet. Chem.* **2013**, *745*, 42–49. **DOI**:10.1016/j.jorganchem.2013.07.033
- E. Tabrizian, A. Amoozadeh, S. Rahmani, RSC Adv. 2016, 6, 21854–21864 DOI:10.1039/C5RA20507G
- J. Safari, M. Ahmadizadeh, J. Taiwan Inst. Chem. Eng. 2017, 74, 14–24. DOI:10.1016/j.jtice.2016.12.010
- C. Wang, B. Lin, G. Qiao, L. Wang, L. Zhu, F. Chu, T. Feng, N. Yuan, J. Ding, *Mater. Lett.* 2016, *173*, 219–222.
   DOI:10.1016/j.matlet.2016.03.057
- B. Yin, X. Zhang, X. Zhang, J. Wang, Y. Wen, H. Jia, Q. Ji, L. Ding, *Polym. Adv. Technol.* 2016, 28, 293–302.
   DOI:10.1002/pat.3886
- 23. K. Thakur, B. Kandasubramanian, *J. Chem. Eng. Data* **2019**, 64, 833–867. **DOI:**10.1021/acs.jced.8b01057
- Y. Zhu, S. Murali, W. Cai, X. Li, J. W. Suk, J. R. Potts, R. S. Ruoff, *Adv. Mater.* 2010, *22*, 3906–3924.
   DOI:10.1002/adma.201001068
- S. Farhadi, M. Hakimi, M. Maleki, Acta Chim. Slov. 2017, 64, 1005–1019. DOI:10.17344/acsi.2017.3731
- W. Yu, L. Sisi, Y. Haiyana. L. Jie, RSC Adv. 2020, 10, 15328– 15345. DOI:10.1039/D0RA01068E
- 27. E. Doustkhah, S. Rostamnia, *J. Colloid Interface Sci.* **2016**, 478, 280–287. **DOI**:10.1016/j.jcis.2016.06.020
- 28. F. Boorboor-Ajdari, E. Kowsari, A. Ehsani, M. Schorowski, T. Ameri, *Electrochim. Acta* **2018**, *292*, 789–804. **DOI:**10.1016/j.electacta.2018.09.177
- M. Tu, K. Wang, S. Bao, R. Zhang, Q. Tan, X. Kong, L. Yu, G. Wu, B. Xu. *J. Colloid Interface Sci.* 2022, 608, 1707–1717.
   DOI:10.1016/j.jcis.2021.10.068
- A. Omidvar, B. Jaleh, M. Nasrollahzadeh, H. RezaDasmeh, *Chem. Eng. Res. Des.* 2017, 121, 339–347.
   DOI:10.1016/j.cherd.2017.03.026
- H. Zhou, S. Bai, Y. Zhang, D. Xu, M. Wang, *Int. J. Environ. Res. Public Health.* 2022, 19, 7584–7602.
   DOI:10.3390/ijerph19137584

- 32. L. H. Choudhury, T. Parvin, *Tetrahedron* **2011**, *67*, 8213–8228. **DOI**:10.1016/j.tet.2011.07.020
- 33. T. Kaur, P. Wadhwa, S. Bagchi, A. Sharma, *Chem. Commun.* **2016**, *52*, 6958–6976. **DOI:**10.1039/C6CC01562J
- N. Kerru, L. Gummidi, S. Maddila, S. B. Jonnalagadda, *Curr. Org. Chem.* 2021, 25, 4–39.
   DOI:10.2174/1385272824999201020204620
- K. Nikoofar, F. M. Yielzoleh, Curr. Org. Synth. 2022, 19, 115– 147. DOI:10.2174/1570179418666210910111208
- 36. Y. Xiao, Q. Zhou, Z. Fu, L. Yu, J. Wang, *Macromolecules* **2022**, 55, 2424–2432. **DOI:**10.1021/acs.macromol.1c02348
- B. Alkan, O, Daglar, S. Luleburgaz, B, Gungor, U. S. Gunay,
   G. Hizal, U. Tunca, H. Durmaz, *Polym. Chem.* 2022, *13*, 258–266. DOI:10.1039/D1PY01528A
- 38. S. S. Sajadikhah, F. Saeedi, H. Dehghan, *Appl. Chem.* **2022**, *17*, 169–178. **DOI:** 10.22075/CHEM.2021.23425.1973
- Z. Li, K. QIU, X. Yang, W. Zhou, Q. Cai, Org. Lett. 2022, 24, 2989–2992. DOI:10.1021/acs.orglett.2c00863
- Yuan, S. Wang, M. Zhao, D. Zhang, J. Chen, J. X. Li, J. Zhang, Y. Song, J. Wang, B. Yu, H. Liu, *Chin. Chem. Lett.* 2020, 31, 349–352. DOI:10.1016/j.cclet.2019.07.019
- S. Lahmidi, H. Anouar, M. Hafi, M. Boulhaoua, A. Ejjoummany, M. Jemli, M. Essassi, J. T. Mague, *J. Mol. Struct.* 2019, 1177, 131–142. DOI:10.1016/j.molstruc.2018.09.046
- 42. P. N. Kalaria, S. C. Karad, D. K. Raval, Eur. *J. Med. Chem.* **2018**, *158*, 917–936. **DOI**:10.1016/j.ejmech.2018.08.040
- A. Ziyaei-Halimehjani, I. N. N. Namboothiri, S. E. Hooshmand, RSC Adv. 2014, 4, 48022–48084.
   DOI:10.1039/C4RA08828J
- A. E. M. Abdallah, R. M. Mohareb, M. H. E. Helal, G. J. Mofeed, *Acta Chim. Slov.* 2021, 68, 604–616.
   DOI:10.17344/acsi.2020.6446
- A. Pourkazemi, N. Asaadi, M. Farahi, A. Zarnegaryan, B. Karami, *Acta Chim. Slov.* 2022, 69, 30–38.
   DOI: 10.17344/acsi.2021.6819
- 46. Y. Huang, J. Liao, W. Wang, H. Liu, H. Guo, *Chem. Commun.* **2020**, 56, 15235–15281. **DOI:**10.1039/D0CC05699E
- Y. Zheng, X. Qi, S. Chen, S. Song, Y. Zhang, K. Wang, Q. Zhang, ACS Appl. Mater. Interfaces 2021, 13, 28390–28397.
   DOI:10.1021/acsami.1c07558
- L. G. do Nascimento, I. M. Dias, G. B. de Souza, L. C. Mourão, M. B. Pereira, J. C. V. Viana, L. M. Lião, G. R. de Oliveira, C. G. Alonso, *New J. Chem.* 2022, 46, 6091–6102.
   DOI:10.1039/D1NJ04686A
- 49. S. Prakash, N. Elavarasan, A. Venkatesan, K. Subashini, M. Sowndharya, V. Sujatha, *Adv Powder Technol.* **2018**, *29*, 3315–3326. **DOI:**10.1016/j.apt.2018.09.009
- S. Akrami, B. Karami, M. Farahi, RSC Adv. 2017, 7, 34315–34320. DOI:10.1039/C7RA06240K
- F. Motamedi-Nia, M. Farahi, B. Karami, R. Keshavarz, *Lett. Org. Chem.* 2021 *18*, 407–414.
   DOI:10.2174/1570178617999200807214103
- K. Fattahi, M. Farahi, B. Karami, R. Keshavarz, *Bulg. Chem. Commun.* 2021, 53, 174–179. DOI: 10.34049/bcc.53.2.5307
- H. Mohamadi-Tanuraghaj, M. Farahi, Monatsh. Chem. 2019, 150, 1841–1847. DOI:10.1007/s00706-019-02471-x

- 54. H. Mohamadi-Tanuraghaj, M. Farahi, RSC Adv. 2018, 8, 27818–27824. DOI:10.1039/C8RA05501G
- J. E. Gholtash, M. Farahi, RSC Adv. 2018, 8, 40962–40967.
   DOI:10.1039/C8RA06886K
- H. Mohamadi-Tanuraghaj, M. Farahi, New J. Chem. 2019, 43, 4823–4829. DOI:10.1039/C8NJ06415F
- 57. B. Karami, M. Farahi, S. Akrami, D. Elhamifar, *New J. Chem.* 2018, 42, 12811–12816. **DOI:**10.1039/C8NJ02699H
- B. Karami, M. Farahi, Z. Banaki, Synlett 2015. 26, 1804–1807.
   DOI:10.1055/s-0034-1380677
- M. Farahi, B. Karami, R. Keshavarz, F. Khosravian, RSC Adv. 2017. 7, 46644–46650. DOI:10.1039/C7RA08253C
- H. Zhang, X. Wang, Na. Li, J. Xia, Q. Meng, J. Ding, J. Lu, RSC Adv. 2018, 8, 34241–34251. DOI:10.1039/C8RA06681G
- O. Metin, S. Aydoğan, K. Meral, J. Alloys Compd. 2014, 585, 681–688. DOI:10.1016/j.jallcom.2013.09.159
- G. Vinodha, P. D. Shima, L. Cindrella, J. Mater. Sci. 2019, 54, 4073–4088. DOI:10.1007/s10853-018-3145-z
- T. Guo, C. Bulin, B. Li, Z. Zhao, H. Yu, H. Sun, H. B. Zhang, *Adsorpt. Sci. Technol.* 2018, 36, 1031–1048.
   DOI:10.1177/0263617417744402
- 64. G. He, W. Liu, X. Sun, Q. Chen, X. Wang, H. Chen, *Mater. Res. Bull.* 2013, 48, 1885–1890.
  DOI:10.1016/j.materresbull.2013.01.038

- S. Feng, Z. Ni, S. Feng, Z. Zhang, S. Liu, R. Wang, J. Hu, J. Radioanal. Nucl. Chem. 2019, 319, 737–748.
   DOI:10.1007/s10967-018-6379-y
- Q. Zhang, H. Su, J. Luo, Y. We, Green Chem. 2012, 14, 201– 208. DOI:10.1039/C1GC16031A
- 67. H. Zhang, H. Li, H. Pan, A. Wang, S. Souzanchi, C. Xu, S. Yang, *Appl. Energy* 2018, 223, 416–429.
  DOI:10.1016/j.apenergy.2018.04.061
- 68. K. Qiao, H. Hagiwara, C. Yokoyama, *J. Mol. Catal. A: Chem.* **2006**, *246*, 65–69. **DOI**:10.1016/j.molcata.2005.07.031
- M. Yadav, K. Y. Rhee, S. J. Park, D. Hui, Compos. B. Eng. 2014, 66, 89–96. DOI:10.1016/j.compositesb.2014.04.034
- S. F. Hojati, A. Amiri, M. Mahamed, Res. Chem. Intermed.
   2020, 46, 1091–1107. DOI:10.1007/s11164-019-04021-w
- 71. X. Yang, W. Chen, J. Huang, Y. Zhou, Y. Zhu, C. Li, *Sci. Rep.* **2015**, *5*, 1–10. **DOI**:10.1038/srep10632
- N. Patel, D. Katheriya, H. Dadhania, A. Dadhania, Res. Chem. Intermed. 2019, 45, 5595–5607.
   DOI:10.1007/s11164-019-03922-0
- L. Zaharani, N. Ghaffari-Khaligh, T. Mihankhah, M. R. Johan, N. A. Hamizi, *Can. J. Chem.* 2020, 98, 630–634.
   DOI:10.1139/cjc-2020-0145
- 74. M. Singh, S. Fatma, P. Ankit, S. B. Singh, J. Singh, *Tetrahedron Lett.* **2014**, *55*, 525–527. **DOI:**10.1016/j.tetlet.2013.11.090

#### **Povzetek**

V prispevku je opisana nova, s sulfonsko kislino funkcionalizirana, ionska tekočina, pripravljena z vezavo 1-(propil-3-sulfonato)-vinilimidazolijevega hidrogensulfata ([(CH<sub>2</sub>)<sub>3</sub>SO<sub>3</sub>HVIm]HSO<sub>4</sub>) na Fe<sub>3</sub>O<sub>4</sub>@GO. Pripravljen heterogeni katalizator je okarakteriziran z XRD, FT-IR, EDX, SEM, VSM in TGA analiznimi tehnikami. Rezultati analiz kažejo, da se je [(CH<sub>2</sub>)<sub>3</sub>SO<sub>3</sub>HVIm]HSO<sub>4</sub> uspešno vezal na površino Fe<sub>3</sub>O<sub>4</sub>@GO in da pripravljen katalizator kaže dobro termično stabilnost. Avtorji so aktivnost katalizatorja raziskali na primeru sinteze triazolo[1,5-a]pirimidinskih derivatov z enostopenjsko trikomponentno reakcijo aktivne metilenske spojine (malononitril ali etil cianoacetat), 3-amin-1*H*-1,2,4-triazola in aril aldehidov, brez uporabe topil. Katalizator je mogoče enostavno in hitro izločili iz reakcijske zmesi s pomočjo zunanjega magneta, ter do sedemkrat reciklirati, brez znatne izgube katalitske aktivnosti.



Except when otherwise noted, articles in this journal are published under the terms and conditions of the Creative Commons Attribution 4.0 International License